

Reactions of Charged Substrates. 4. The Gas-Phase Dissociation of (4-Substituted benzyl)dimethylsulfoniums and -pyridiniums

Neil Buckley,* David Maltby, Alma L. Burlingame, and Norman J. Oppenheimer

The Department of Pharmaceutical Chemistry, School of Pharmacy, S-926, Box 0446, The University of California, San Francisco, California 94143-0446

Received July 13, 1995 (Revised Manuscript Received January 25, 1996[®])

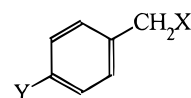
The relative rates for the gas-phase dissociation $RX^+ \rightarrow R^+ + X^\ominus$ of five (4-Y-substituted benzyl)-dimethylsulfoniums (Y = MeO, Me, H, Cl, and NO₂) and 24 (4-Y-substituted benzyl)-3'-Z-pyridiniums (complete series for Z = CN, Cl, CONH₂, and H, and 4-methoxy- and 4-nitrobenzyls for Z = F and CH₃CO) were measured using liquid secondary ion mass spectrometry. The Hammett plot (vs $\delta\Delta G^\ominus$ or σ^+) is linear for the sulfoniums, but plots for the four pyridinium series have a drastic break between the 4-Cl and 4-NO₂ substrates. Brønsted-like plots for the pyridiniums show a strong leaving group effect only for 4-nitrobenzyls. An analysis of these linear free energy relations with supporting evidence from semiempirical computations suggests that collisionally activated pyridinium substrates dissociate by two pathways, direct dissociation and through an ion-neutral complex intermediate. Comparison of these results with results for the solution reactions of some of these compounds shows that the mechanism is different in the gas and solution phases. Sufficient experimental data are not available to assign a mechanism for dissociation to the sulfonium series, but computational results show characteristics of a direct dissociative mechanism.

Introduction

As part of continuing studies on the cleavage of the nicotinamide-ribose bond in β -nicotinamide adenosine dinucleotide (NAD⁺),¹ we recently reported the results of a study of the gas-phase dissociation of a series of 2'-substituted β -nicotinamide arabinosides.² The relative rates of dissociation, measured by tandem positive-ion liquid secondary ion mass spectrometry (LSIMS), follow the Taft equation and correlate with the relative rates for the dissociation in water.³ An analysis of the product ratios and the AM1 energy profiles for dissociation of the nicotinamide-ribose bond shows that an ion-neutral complex (INC, used to designate the gas-phase intermediate) is involved. Rearrangements within the INC that occur after the rate-limiting step are readily explained by the relative energies of the possible products. The system is complex, but easily understood.

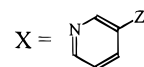
A large part of our recent efforts to understand NAD⁺ hydrolysis in detail has centered on an extensive study of the mechanisms of substitution of charged benzyl substrates.^{4–6} The hydrolysis and nucleophilic substitution reactions of benzyl dimethylsulfoniums (**1**) (Chart 1) have been interpreted in terms of an ion-dipole complex (IDC, used to designate the solution intermediate) mechanism.⁷ The kinetics of the nucleophilic substitution reactions of (4-methoxybenzyl)dimethylsulfonium (**1a**) with a large number of nucleophiles and added

Chart 1



Y = MeO Me H Cl NO₂
a b c d e

X = SMe₂
1



Z = CN CONH₂ H Cl F Ac
2 3 4 5 6 7

salts have been measured.⁴ **1a** reacted only with nucleophiles of intermediate hardness and not with hard or soft nucleophiles. The hydrolysis reaction is complicated by the establishment of an equilibrium among starting material and products,⁵ but it is clear from the kinetics and the selectivities that the reaction is mixed S_N1/S_N2 under constant ionic strength. Kevill and his colleagues⁸ reached the same conclusion independently. Hammett plots for the azide reaction and hydrolysis show distinct breaks but are not V-shaped.

The kinetics of the reaction between azide and the benzylpyridinium substrates **2–4a–e** in water have been measured.⁶ The reactions are strictly S_N2 with no evidence for an IDC intermediate, despite the fact that the values of β_{LG} are quite large (–1.4 to –1.6). The rates for the hydrolysis reactions of **2a–e** are quite slow compared with the rates for the azide reaction, but the rates of the two reactions are comparable for **3a–e**. Hammett plots for hydrolysis of **2–3a–e** are linear but

* Abstract published in *Advance ACS Abstracts*, March 15, 1996.

(1) (a) Johnson, R. W.; Marshner, T. M.; Oppenheimer, N. J. *J. Am. Chem. Soc.* **1988**, *110*, 2257–2263. (b) Handlon, A. L.; Xu, C.; Müller-Steffnar, H.; Schuber, F.; Oppenheimer, N. J. *J. Am. Chem. Soc.* **1994**, *116*, 12087–12088.

(2) Buckley, N.; Handlon, A. L.; Maltby, D.; Burlingame, A. L.; Oppenheimer, N. J. *J. Org. Chem.* **1994**, *59*, 3609–3615.

(3) Handlon, A. L.; Oppenheimer, N. J. *J. Org. Chem.* **1991**, *56*, 5009–5010.

(4) Buckley, N.; Oppenheimer, N. J. Submitted. Some results have been presented in ref 5.

(5) Buckley, N.; Oppenheimer, N. J. *J. Org. Chem.* **1994**, *59*, 5717–5723.

(6) Buckley, N.; Oppenheimer, N. J. Submitted.

(7) For reactions of **1a,c**: Sneen, R. A.; Felt, G. R.; Dickason, W. C. *J. Am. Chem. Soc.* **1973**, *95*, 638–639. For the ion-pair mechanism for neutral substrates: Sneen, R. A. *Acc. Chem. Res.* **1973**, *6*, 46–53.

(8) Kevill, D. N.; Ismail, N. H. J.; D'Souza, M. J. *J. Org. Chem.* **1994**, *59*, 6303–6312.

have different slopes. While **4a,e** react very slowly with azide, **4b–d** did not react with either water or 1.7 M azide after 6 months at 96 °C.⁶

In contrast, Katritzky and his colleagues⁹ found that the reactions between 4-substituted benzyl substrates with highly arylated pyridine leaving groups (LGs) and neutral amine nucleophiles in solvent chlorobenzene exhibited borderline kinetic behavior for the 4-methoxybenzyl compounds but not for substrates with less electron-donating substituents. These results were interpreted in terms of an IDC mechanism, which was supported by the results of ion cyclotron resonance (ICR) experiments^{10,11} and a computational study.¹²

These wildly different results prompted us to examine the collisionally activated gas-phase dissociation of **1a–e** and four series of benzylpyridiniums (**2–5a–e**) with tandem LSIMS. Hammett and Brønsted-like plots based on relative rates for gas-phase and solution dissociation of **1a–e** and **2–5a–e** show differences among and between the two series in both phases. These results were used to analyze the kinetics of the gas-phase reaction. It appears that **1a–e** may react by direct dissociation and that **2–5a–d** react through direct dissociation and INC mechanisms, while **2–5e** react only through direct dissociation.

Experimental Section

General. All chemicals and solvents were obtained from Aldrich and used without further purification. NMR spectra were recorded in D₂O at 300 MHz.

Synthesis. All substrates were prepared by mixing 1 equiv of the appropriate benzyl chloride with 1.1 equiv of either SMe₂ or the appropriate pyridine in chloroform at ambient temperature. Reactions were followed by TLC (silica, neat chloroform) until all chloride had disappeared. The chloroform layer was extracted with water, and the aqueous layer was back-extracted extensively with chloroform and then with ether to give water-white solutions. Rotary evaporation at reduced pressure with repeated flashing with ethanol to remove traces of water gave products that were >95% pure by proton NMR. For several of the 3-cyanopyridine substrates, the alkylation was performed by adding the chloride to a melt of the pyridine, which was held in a drying oven at ca. 110 °C for 10–20 min. After cooling, the (usually dark brown) solid was dissolved in water and carried through the extraction procedure. Heating the water layer with Norit A and filtering through a pad of Filtre-Aid, followed by evaporation, gave pure compound. All compounds are known with various counterions and were characterized only by proton NMR and LSIMS.

LSIMS Spectra. Tandem mass spectra were recorded under identical conditions in the positive ion mode on a four-sector Kratos Concept II HH mass spectrometer fitted with an optically coupled 4% diode array detector on MS II. Substrates were sputtered from a glycerol matrix with Cs⁺ (18 keV), and the molecular ion was sorted into MSII where fragmentation was induced by collisional activation with helium (13 eV). Seven to 10 determinations were collected and averaged in the computer (<5% error).

Computational Methods. Semiempirical computations in MNDO, AM1, and PM3¹³ were performed on a 486/66 (16 MB

Table 1. Log [R⁺/(R⁺ + M⁺)] for the Gas-Phase Dissociation of (4-Y-benzyl) dimethylsulfoniums and 3-Z-pyridiniums

LG/Y	MeO	Me	H	Cl	NO ₂
SMe ₂	-0.78	-1.06	-1.23	-1.14	-1.71
3-CN-Py	-0.95	-1.05	-1.14	-1.16	-1.83
3-Cl-Py	-0.95	-1.07	-1.15	-1.21	-1.89
nicotinamide	-1.00	-1.11	-1.21	-1.20	-2.05
3-H-Py	-0.99	-1.25	-1.29	-1.31	-2.30

RAM) with Releases 3.0 and 4.0 of the Hyperchem software using methods described elsewhere.²

To construct the energy profiles for **5a–e**, the benzyl-C7–pyridine bond length was increased in steps from the initial length of 1.49–1.52 Å using the restraint function to a final restraint force constant of 10⁵. Each structure was minimized completely with no restraint other than the reaction coordinate. Transition state structures were refined until a single negative (imaginary) frequency¹⁴ was obtained using the Vibrational Analysis subroutine. Energies of the carbenium ions were calculated after manual removal of the LG from the INC. Stabilities of the INCs were assessed by removing the reaction coordinate constraint from the structure corresponding to the minimum in the energy profile and re-minimizing.

For the norcaradienylcarbenium ions (**9**), structures were formed from the corresponding benzylcarbenium ions (**8**) and minimized in MM+ before being fully minimized in AM1.

Results

Experimental. LSIMS Results. For all compounds, LSIMS spectra obtained in MSII had two peaks that corresponded to the parent molecular ion M⁺ and the respective benzylcarbenium ion R⁺, consistent with heterolytic cleavage. The relative rates for dissociation were obtained as the ratio of the relative abundances [R⁺/(R⁺ + M⁺)], with M⁺ ≡ 100. These values are summarized in Table 1. Because the average error in the measurements is <5%, in plots of these data the error bars are within the symbols.

Spectra for the 4-nitropyridinium compounds **2–5e** had additional peaks, not found in any spectrum for the **2–5a–d** compounds, that corresponded to the respective pyridine radical-cation and its decomposition products, consistent with homolytic cleavage. The relative abundances of these species were less than or equal to those for the carbenium ion (1–2% of M⁺). These small yields have insignificant effects on the relative rates.

Each sulfonium spectrum had a very small peak at *m/z* 61 that may correspond to the sulfonium product formed in a four-centered hydride reduction reaction, ArCH₂SMe₂⁺ → ArCH₃ + [CH₂=SMe]⁺. No pyridinium spectrum had a peak corresponding to 3-Z-PyH⁺.

Linear Free Energy Relations (LFERs). Because it is advisable to use a scale derived from gas-phase data, Hammett plots of log [R⁺/(R⁺ + M⁺)] for **1a–e** (Figure 1) and **2–5a–e** (Figure 2) were constructed vs $\delta\Delta G^\circ_{t-cumyl}$ for the gas-phase reaction 4-Y-C₆H₄C(Me)=CH₂ + H⁺ ⇌ 4-Y-C₆H₄CMe₂⁺; values have been summarized by Taft and Topsom.¹⁵ (The $\delta\Delta G^\circ_{t-cumyl}$ and σ^+ scales correlate well; for substituents **a–c,e**, $r = 0.9999$ with a slope of 14.) The plots are clearly different, with good linearity for the sulfoniums and a distinct break for the pyridiniums. The slopes “ γ^+ ” are -0.042 ($r = 0.9999$ with the point for **1d** excluded), $r = 0.9964$ with the point for **1d** included) for **1a–e**, and -0.020 ($r = 0.983$), -0.022 ($r =$

(9) Reviewed in: Katritzky, A. R.; Brycki, B. E. *Chem. Soc. Rev.* **1990**, *19*, 83–105 and elsewhere.

(10) Katritzky, A. R.; Watson, C. H.; Dega-Szafran, Z.; Eyley, J. R. *J. Am. Chem. Soc.* **1990**, *112*, 2471–2478.

(11) Katritzky, A. R.; Malhotra, N.; Dega-Szafran, Z.; Savage, G. P.; Eyley, J. R.; Watson, C. H. *Org. Mass Spectrom.* **1992**, *27*, 1317–1321.

(12) Katritzky, A. R.; Malhotra, N.; Ford, G. P.; Anders, E.; Tropsh, J. G. *J. Org. Chem.* **1991**, *56*, 5039–5044.

(13) AM1: Dewar, M. J. S.; Zoebisch, E. G.; Healy, E. F.; Stewart, J. J. P. *J. Am. Chem. Soc.* **1985**, *107*, 3902–3909. PM3: Stewart, J. J. P. *J. Comput. Chem.* **1989**, *10*, 209–220, 221–264.

(14) McIver, J. W., Jr.; Komornicki, A. *Chem. Phys. Lett.* **1971**, *10*, 303–306.

(15) Taft, R. W.; Topsom, R. D. *Prog. Phys. Org. Chem.* **1987**, *16*, 2–83.

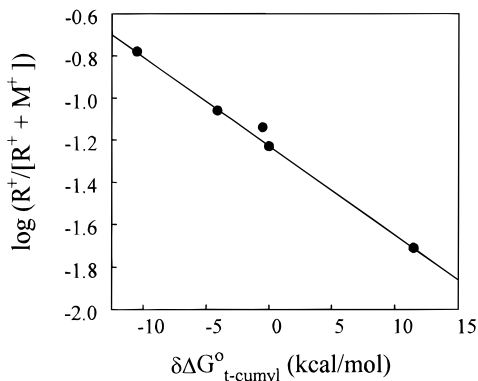


Figure 1. Plot of the LSIMS data for **1a–e** vs the relative free energy for gas-phase formation of *tert*-cumylcarbenium ions. The point off the line is for **1d**; the regression line is for the other points with a slope of “ γ^+ ” = -0.042 ($r = 0.9999$). With the point for **1d** included, $r = 0.996$. Left to right the points are for **1a**, **1b**, **1d**, **1c**, and **1e**.

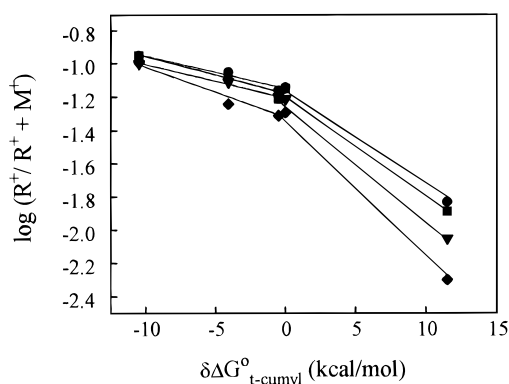


Figure 2. Plots of the LSIMS data for **2a–e** (●), **3a–e** (■), **4a–e** (▼), and **5a** (◆) vs the relative free energy for gas-phase formation of *tert*-cumylcarbenium ions. Left to right the points are for **a–e**. The slopes of “ γ^+ ” are as follows: **2a–d** = 0.020 ($r = 0.98$), **3a–d** = 0.022 ($r = 0.96$), **4a–d** = 0.020 ($r = 0.996$), and **5a–d** = 0.030 ($r = 0.97$).

0.960), -0.020 ($r = 0.996$), and -0.030 ($r = 0.970$) for **2a–d**, **3a–d**, **4a–d**, and **5a–d**, respectively. Thus, as expected, the rates decrease with the basicity of the pyridine. (Hammett plots for **1a–e** and **2a–d** against σ^+ are shown in Figures 6 and 7 with the data for hydrolysis.)

For Brønsted plots of the experimental data for the four complete series of pyridiniums, with additional points for **6a,e** and **7a,e**, $\log [R^+/(R^+ + M^+)]$ was plotted vs values of $\delta\Delta G^{\circ}_{Py}$ for the gas-phase protonation of pyridines¹⁵ (Figure 3). The value for nicotinamide is not available, but was estimated by interpolation against solution pK_a values, which assumes that the effects are constant between the gas phase and solution. For **2–7a** and **2–5b–d**, plots are grouped together and have small slopes; for **2–7e**, however, there is a definite slope, which corresponds to the pattern seen for the spread of points for **2–5e** in Figure 2.

Computational. Pyridiniums. Because there is little effect of the LG on the experimental data, complete energy profiles (Scheme 1) were calculated only for **4a–e**, which is the simplest pyridinium computational system. Our results agree with those reported by Katritzky et al.¹² that the PM3 energy profiles for pyridiniums have no distinct transition states (not shown; the profile for **4c** has been reported²). In AM1, profiles for **4a–d** had

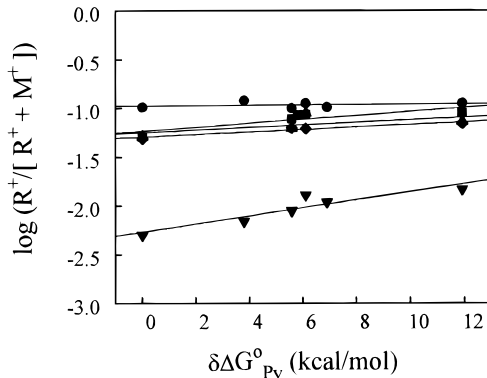


Figure 3. Plots of the LSIMS data for **2–7a** (●), **2–5b** (■), **2–5c** (▲), **2–5d** (◆), and **2–7e** (▼) vs the relative free energy for gas-phase protonation of the respective pyridine LGs. Slopes for the **a–d** compounds are 0.01 – 0.04 and for the **e** compounds is 0.12 .

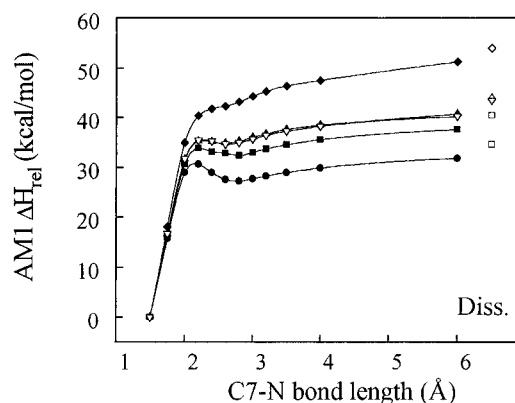
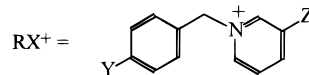
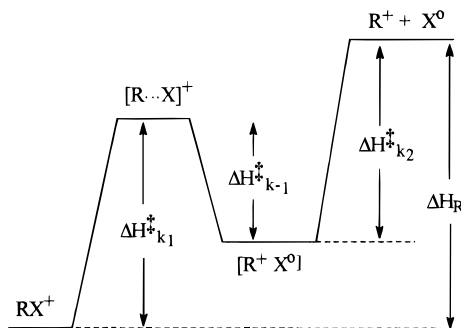


Figure 4. AM1 energy profiles for the gas-phase dissociation of **5a** (●), **5b** (■), **5c** (▲), **5d** (▼, shown open for clarity), and **5e** (◆). The open symbols are values for ΔH_R for complete dissociation of the carbenium ion and LG. The bond length at the transition state is relatively constant at ca. 2.2 \AA .

Scheme 1



$$\Delta H_{k_1}^{\ddagger} = \Delta H_f[R\cdots X^{\ddagger}] - \Delta H_f[RX^+]$$

$$\Delta H_{k_{-1}}^{\ddagger} = \Delta H_f[R\cdots X^{\ddagger}] - \Delta H_f[R + X^0]$$

$$\Delta H_{k_2}^{\ddagger} = (\Delta H_f[R^+] + \Delta H_f[X^0]) - \Delta H_f[R + X^0]$$

$$\Delta H_R = (\Delta H_f[R^+] + \Delta H_f[X^0]) - \Delta H_f[RX^+]$$

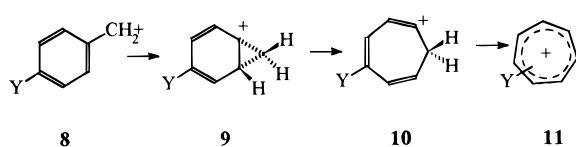
distinct transition states, but the profile for **4e** was consistent with dissociation without an INC (Figure 4). We calculated several profiles for various pyridiniums in

Table 2. AM1 Enthalpies of Formation for the Gas-Phase Dissociation of (4-Y-benzyl)pyridiniums (kcal/mol)^a

	starting structure	transition state	ion-dipole complex	carbenium ion
MeO	170.3	201.0	197.6	173.0
Me	201.0	234.8	233.4	209.6
H	209.8	245.1	244.6	221.9
Cl	204.5	239.9	239.1	216.1
NO ₂	221.8			243.9

^a ΔH_f pyridine = 31.9 kcal/mol.**Table 3. AM1 Activation Enthalpies and Enthalpies of Reaction for the Gas-Phase Dissociation of (4-Y-benzyl)pyridiniums (kcal/mol)^a**

	$\Delta H^\ddagger k_1$	$\Delta H^\ddagger k_{-1}$	$\Delta H^\ddagger k_2$	ΔH_R
MeO	30.7	3.4	7.3	34.6
Me	33.8	1.4	8.2	40.5
H	35.5	0.8	9.2	44.0
Cl	35.4	0.5	8.9	43.5
NO ₂				54

^a Designations of rate constants refer to Scheme 1.**Scheme 2**

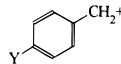
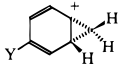

MNDO and found that the energies were several kcal/mol lower than found for AM1; the MNDO profile for **4c** has been reported.² Values for the various AM1 energies are listed in Table 2; the activation values obtained from these energies are summarized in Table 3.

Sulfoniums. No distinct transition states were found in the PM3 or AM1 reaction profiles for **1a–e** (not shown).

Tropyliums. Benzylcarbenium ions (**8**) may rearrange to tropylium carbenium ions (**11**) in the gas phase (Scheme 2).¹⁶ Values of ΔH^\ddagger calculated for heterolytic cleavage of the benzyl methylene–pyridine bond would not be affected by rearrangements that take place in the INC after bond cleavage, but rates for the recombination reaction would be affected because the affinity of tropylium and benzylcarbenium ions for nucleophiles are different. Thus, the stabilities of the carbenium ions is of some importance.

Katritzky^{10,11} measured the appearance potentials (APs) for carbenium ions formed by collisional activation of laser-desorbed (4-Y-substituted benzyl)pyridiniums. Because of a correlation between the APs and AM1 values of ΔH_R for benzylcarbenium, but not for tropylium carbenium, ions formed from simple, unhindered pyridiniums, Katritzky¹⁰ argued that no benzyl-to-tropylium rearrangement took place within the INC (although the 4-Br and 4-Cl compounds may have undergone this rearrangement). For highly hindered 4-Y-substituted benzyl substrates (Y = MeO, Me, H, F, Cl, NO₂) with 2,4,6-triphenylpyridinium LGs, however, he¹¹ argued that the measured APs and the calculated AM1 ΔH_R were consistent with benzyl-to-tropylium rearrangements within the INC. While the correlations between AP and the AM1 ΔH_R for dissociation to either tropylium or benzyl-

Table 4. AM1 ΔH_f and ΔH_R , from the Pyridiniums, of (4-Y-substituted benzyl)carbenium (4-Y-substituted norcaradienyl) and 4-Y-Substituted Tropylium Carbenium Ions (kcal/mol)

Y			
	8	9	11
ΔH_f			
MeO	173.0	173.0	167.7
Me	209.6	262.4	200.7
H	221.9	271.3	210.3
Cl	216.1	269.2	207.9
NO ₂	243.9	291.3	233.3
ΔH_R			
MeO	34.6	34.6 ^a	29.3
Me	40.5	93.3	31.6
H	44.0	93.4	23.4
Cl	43.5	96.6	35.3
NO ₂	54.0	101.4	43.9

^a Reverts to the benzylcarbenium ion upon minimization.

carbenium ions are not good (Figure 1 of ref 11), using the published values for the APs and computed ΔH_R , we found that the correlation is measurably better for the benzyl energies ($r = 0.90$) than for the tropylium energies ($r = 0.82$) in plots of AP vs ΔH_R (not shown). If the points for 4-NO₂ and 4-H are ignored, the correlation coefficients are 0.94 and 0.95 for benzyls and tropyliums, respectively, which reflects the effects of the substituents on the stabilities of the carbenium ions, not on the ability of the benzyls to rearrange. By themselves, these fits of data and computed energies show that the benzylcarbenium ions are stable within the INC for both groups of pyridine LGs.

Dewar and his colleagues have calculated the barriers to isomerization of benzyl-¹⁷ and substituted benzylcarbenium¹⁸ ions into the corresponding tropylium carbenium ions through the sequence shown in Scheme 2. In MINDO/3, the barrier for **8** → **11** is ca. 33 kcal/mol. While we did not determine the activation barriers, we calculated ΔH_R in AM1 (Table 4) for the conversion **8** → **9**. The (4-methoxynorcaradienyl)carbenium ion (**9a**) reverts to the (4-methoxybenzyl)carbenium ion upon minimization; the other compounds have values of ΔH_R 4- to 6-fold greater than ΔH^\ddagger for dissociation of the INC into the carbenium ion and the LG. The sequence **9** → **10** → **11** would require more energy; ΔH_f for the tropyliums in PM3 are 10–20 kcal greater than the corresponding MINDO/3 values,^{18a} which suggests that the total energy of conversion would be 40–50 kcal/mol, assuming crudely—simple additivity between the methods. If benzylcarbenium ions other than the 4-MeO— isomerized to tropylium ions in our systems, a break between the energies for **1–5a** and the other compounds would be expected; there is none. Note that the break at the 4-NO₂ compound for the pyridiniums **2–5** is not the result of an isomerization. First, if this were the case the line in

(17) Cone, C.; Dewar, M. S. J.; Landman, D. *J. Am. Chem. Soc.* **1977**, *99*, 372–376.(18) (a) Dewar, M. J. S.; Landman, D. *J. Am. Chem. Soc.* **1977**, *99*, 4633–4639. (b) Dewar, M. J. S.; Landman, D. *J. Am. Chem. Soc.* **1977**, *99*, 7439–7445.(16) (a) Kuck, D. *Mass Spectrom. Rev.* **1990**, *9*, 187–233. (b) For an extensive review of earlier work, see: Bursey, J. T.; Bursey, M. M.; Kingston, D. G. I. *Chem. Rev.* **1973**, *73*, 191–234.

Figure 2 should break up, not down. Second, it has been estimated that the energies for the isomerization of the (4-methoxybenzyl) and (4-nitrobenzyl)carbenium ions are the same.^{16a} Thus, we are confident that the benzylcarbenium ions do not rearrange in the sulfonium and pyridinium INCs under our experimental conditions.

Discussion

In the gas phase, a molecule with sufficient internal energy may vibrate so violently that the weakest bond is broken, producing two fragments by either homolytic or heterolytic cleavage.^{19–23} Heterolytic cleavage of positively charged molecules produces a cation and a neutral, with the charge borne by the less polarizable fragment²⁰; the positive charge will switch fragments upon dissociation, $RX^+ \rightarrow R^+ + X^\circ$, as found for all compounds studied here.²⁴ Molecules with sufficient energy may fling the fragments sufficiently far apart ($>10 \text{ \AA}$) that mutual attraction is overcome and they do not recombine. Completely dissociated products fall into potential wells, separated from RX^+ by the Longevin transition state.²² If there is not sufficient energy to cause complete dissociation, an intermediate INC $[R^+ X^\circ]$ may form.^{20,22}

The general criterion that must be met for $[R^+ X^\circ]$ to be an intermediate is that both fragments must be able to rotate about an axis orthogonal to the interfragment axis, a maneuver prevented in the parent by the R–X bond.^{22,23} The fate of the INC depends on a number of factors related to the free rotation—or lack of it—of the fragments in either of two “critical configurations” determined by the “density of states,” kinetic-statistical quantities from RRKM theory.²⁵ In general, however, there are three possibilities. One is dissociation into R^+ and X° , which can occur if the energy associated with the internal degrees of freedom is converted into sufficient motion along the reaction coordinate that the attractive forces are overcome. The second is recombination to RX^+ . In order for this to occur, a “locked rotor” critical configuration must be achieved in which the HOMO of X and LUMO of R^+ are aligned properly to form a covalent bond.²² The locked rotor critical configuration does not correspond to a saddle point on a potential energy surface. Because of free translation of the ion and neutral, the fragments may exist in what Morton has called an “orbiting critical configuration.” Formation of the locked rotor occurs with loss of translational entropy, and there is an entropic “bottleneck” to recombination; attractive forces create an enthalpic barrier to complete dissociation of the fragments. If $[R^+ X^\circ]$ can exist with a nonzero lifetime between the two critical configurations, it is an INC. This intermediate may, but does not have to, correspond to a minimum on a potential energy surface.²³

The third possibility is reactions within the INC and between the ion and neutral in the INC. R^+ may

isomerize to a more stable species (through a 1,2 hydride shift, $MeCH_2CH_2^+ \rightarrow Me_2HC^+$)¹⁹ and/or there may be a proton transfer from the cation to the base (such as the commonly observed β -elimination $Me_2HC^+ + X \rightarrow CH_2=CHMe + XH^+$).^{19,26} Proton transfer is less endothermic than dissociation.²⁶ Both processes occur and provide evidence for the existence of an INC intermediate.^{19,21,26} The conclusions are bolstered by isotope labeling and stereochemical studies on gas-phase reactions, including Morton's work collecting and analyzing neutral hydrocarbon products.¹⁹ In the absence of this daunting task, however, it is often sufficient to show that proton transfer takes place, signaled by the presence of XH^+ among the products.^{22,26}

In our earlier study of the collisionally activated, gas-phase dissociation of 2'-substituted β -nicotinamide arabinosides,² protonated nicotinamide was a prominent product formed by abstraction of a proton from the 5'-OH in all compounds and from 2'- β -NH₂ and 2'- β -OH groups in two others, which established that the reaction proceeded through an INC. With one exception, this diagnostic reaction is not available in the benzylsulfonium or -pyridinium systems. It is possible that a methyl proton could be abstracted from the 4-Me carbenium ion to form the quinoid *p*-xylylene, but no protonated pyridine or sulfonium is detected in any series. As noted in the Results, it is doubtful that any of the benzylcarbenium ions rearrange to tropylium carbenium ions under our reaction conditions. In the absence of this classic evidence we must deduce from the available data whether or not an INC can be identified in either the sulfonium or pyridinium series.

For the sulfoniums, it is not possible to choose between direct dissociation and an INC mechanism. The fact that the plot of $\log k_{rel}$ vs $\delta\Delta G^\circ$ (or σ^+) is linear (Figure 1) suggests only that the mechanism is the same within the series and that there is considerable carbenium ion character, which would be characteristic of either a direct dissociation or INC mechanism.

For the pyridiniums, however, it is possible to speculate about mechanism based on the shape of the gas-phase Hammett (Figure 2) and Brønsted-like plots (Figure 3). The Hammett plot has a break down, which is usually interpreted as the signature for a change in rate-limiting step, not in mechanism.²⁷ By itself, this break implies that there are at least two kinetically significant steps in the reaction.²⁸ The Brønsted plots show that there is no LG effect for the 4-MeO substrates, a slight effect for the 4-Me, 4-H, and 4-Cl substrates (although the values upon which they are based are within or near the 5% error), and a marked effect for the 4-NO₂ substrates that follows pyridine basicity (bond strength) and is consistent with rate-limiting cleavage of the R–X⁺ bond.

(26) Bowen, R. D. *Acc. Chem. Res.* **1991**, *24*, 364–371 and references cited therein for the work of the Cambridge group.

(27) Leffler, J. E.; Grunwald, E. *Rates and Equilibria of Organic Reactions*; Wiley: New York, 1963; pp 190–191 (Dover edition, 1989).

(28) The often-stated assumption that a break down in a Hammett plot signals a change in rate-limiting step assumes *a priori* that there is only a single process involved. In the majority of cases where this has been documented for solution reactions, it is of course true. There is no good theoretical or practical reason to suppose, however, that this is *generally* true. For instance, a break up may signal either a change in mechanism (see refs 5 and 31) or a change in the structure of the activated complex (see ref 33). There is no reason to suppose that the break down should be any different. All that is required for any break in a Hammett plot are two kinetically distinguishable steps irrespective of whether or not they represent a single mechanism in which k_{obsd} is related to several individual rate constants (and their relative rates) or represent two mechanisms with different rate constants that contribute to k_{obsd} .

(19) Morton, T. H. *Tetrahedron* **1982**, *38*, 3195–3243.

(20) McAdoo, D. J.; Morton, T. H. *Acc. Chem. Res.* **1993**, *26*, 295–302.

(21) Kondrat, R. W.; Morton, T. H. *J. Org. Chem.* **1991**, *56*, 952–957.

(22) Morton, T. H. *Org. Mass. Spectrom.* **1992**, *27*, 353–368.

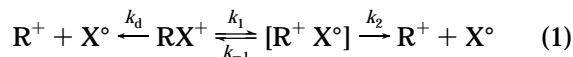
(23) Kondrat, R. W.; Morton, T. H. *Org. Mass. Spectrom.* **1991**, *26*, 410–415.

(24) That the (4-nitrobenzyl)pyridiniums also undergo homolytic cleavage is not surprising, because of all possible carbenium ions that can be produced, only the (4-nitrobenzyl)carbenium will not be stabilized by resonance, while the 4-nitrobenzyl radical would be.

(25) Forst, W. *Theory of Unimolecular Reactions*; Academic Press: New York, 1973.

Under the conditions of our experiment, in which the internal energies of all RX^+ are assumed to have a Boltzmann distribution around the average energy of the collision gas, 13 eV, there are populations of RX^+ with sufficient energy to dissociate directly or to form INCs; there are also populations that do not have sufficient internal energy to undergo bond cleavage. Kondrat and Morton²³ have shown that steady-state kinetics can be used to analyze relative rates for the separate processes under these conditions. Their approach is not directly applicable to our system, however, because we obtain a single detectable product, R^+ .

Possible pathways are given in eq 1. Each channel will be considered separately. Direct dissociation alone (k_d



pathway) is not consistent with the Hammett plot. Formation of the INC alone with partitioning between dissociated products and starting material is a multistep process; steady-state treatment gives $k_{\text{obsd}} = k_1 k_2 / (k_{-1} + k_2)$. If $k_2 > k_{-1}$, $k_{\text{obsd}} = k_1$, a pathway kinetically indistinguishable from the k_d pathway and inconsistent with the Hammett plot. (As shown below, this assumption does not fit the AM1 energy.) If $k_2 \sim k_{-1}$, then k_{obsd} is either $k_1/2$, which is not probable, or $Kk_2/2$. The case in which $k_{-1} > k_2$ yields $k_{\text{obsd}} = Kk_2$. This is the most reasonable case based on the assumption that the barrier to recombination is smaller than the barrier to dissociation of the INC. Both this and the $Kk_2/2$ case, however, are difficult to rationalize in terms of the Hammett and Brønsted plots. Assuming that k_2 would be relatively constant across the series (see below), k_{obsd} will vary based on the value of K , which is mediated by obverse (and compensating) effects of the stability of R^+ on k_1 —decreasing with a decrease in stability—and k_{-1} —increasing with a decrease in stability. It seems reasonable that K should decrease smoothly over the series just as the equilibrium protonation of 2-(4-Y-phenyl)propenes, the basis of the gas-phase $\delta\Delta G^\ominus$ scale for *tert*-cumyl carbenium ions,¹⁵ changes smoothly and continuously over a wide range of Y. It is difficult to rationalize the discontinuity in the Hammett plot and the dependence on the leaving group for the 4-NO₂ substrates in terms of this continuous monotonic rate expression. Thus, attempting to fit the results into a mechanism involving only INC intermediates is unsuccessful.

Considering the entire mechanism in eq 1 and applying a steady state treatment yields $k_{\text{obsd}} = k_d + k_1 k_2 / (k_{-1} + k_2)$. With the assumption that $k_{-1} > k_2$ for the reasons give above, $k_{\text{obsd}} = k_d + Kk_2$. Because the mass of the parents does not vary greatly and because a majority of the internal energy imparted to RX^+ by collisional activation is released in bond breaking,²³ k_d should remain relatively constant over the series and changes in k_{obsd} should be dominated by Kk_2 when $Kk_2 > k_d$. The Brønsted plots in Figure 2 show no or little effect of the LG for the MeO, Me, H, and Cl substrates, which suggests that this condition is satisfied. Under the assumption that k_2 is relatively constant, as R^+ becomes less stable changes in the values of k_1 and k_{-1} , but especially in k_{-1} , cause the value of K to diminish to the point that $k_d > Kk_2$ for the 4-NO₂ substrate, which could account for the break in the Hammett plot and the leaving group dependence exhibited in the Brønsted

plots—an uncompensated decrease in k_d that parallels R–Py⁺ bond strength. The fact that the relative abundance of the (4-nitrobenzyl)carbenium ion is so low suggests that the INC mechanism is dominant for the other substrates.

In his reviews on these matters,^{19,20,22} Morton has pointed out that gas-phase dissociative reactions do not require that the intermediates are energy minima on potential energy surfaces, a condition that *may be present* but *is not required* by RRKM theory.²⁵ In addition to the INC, three other possible intermediates may be associated with potential energy surfaces.²² One is a hydrogen-bonded intermediate, the second is a π complex in analogy with the electrophile–aromatic complexes that are thought to precede the Wheland intermediate in electrophilic aromatic substitution reactions, and the third is a potential energy minimum associated with a long bond extension.

We have examined these factors by computing in AM1 the potential energy surfaces for reaction of **4a–e**. (The barriers for the various rate constants are given in Scheme 1.) The results confirm—but do not prove—the assumptions made above concerning the relative barriers for partitioning of the INC (Tables 3 and 4 and Figure 4). The energy profiles show distinct transition states for all but the 4-NO₂ substrate **4e**, which has a slight “hump” in the curve but no distinct minimum. For **4a–d**, values of ΔH^\ddagger are high and relatively constant for k_1 and low and relatively constant for k_2 but decrease progressively for k_{-1} (Table 3), consistent with the assumptions made above. Because of the absence of a distinct minimum for the INC, these values are not available for **4e**. For **4a–d**, the values of $\log K$ estimated from the computed $\Delta\Delta H^\ddagger = \log k_1/k_{-1}$ values give a linear plot vs $\delta\Delta G^\ominus$ ($r = 0.998$, not shown), consistent with the proposed mechanism.

The R–Py⁺ bond length is ca. 2.8 Å in the constrained structures that give an energy minimum consistent with an INC (Figure 4). If the bond length constraint is removed in the INCs for **4a–d** (**4iii**) and the resulting structures are minimized, all remain stable species, consistent with the presence of an enthalpic barrier to collapse. The **4e** “INC”, however, spontaneously collapses back to the starting structure (**4i**) upon minimization. Moreover, minimizing the π complex between the cation and the pyridine (**4ii**), formed by rotating the latter 90° about its center of mass, leads directly back to the INC for **4a–d**; the **4e** “INC” collapses back to the starting structure (Scheme 3). Rotation of the pyridine by 180° about its center of mass—N lone pair pointing 180° away from the carbenium ion with a benzyl–pyridine separation of ca. 3.6 Å—and minimizing in AM1 produces a stable structure (**4iv**) that could contribute to an enthalpic bottleneck against collapse of the INC. Hydrogen-bonded structures are not found in any INC. Thus, within the limits of the semiempirical methodology, these structures appear to be type 1 INCs.²²

In a very recent study of the gas-phase dissociation of protonated *tert*-butyl alkyl ethers, Morton and his colleagues²⁹ found that [*t*-Bu⁺ HOR] did not correspond to a minimum on the potential energy surface calculated at the 3-21G//3-21G level of theory. Because the mechanisms leading to various products require the existence of an INC, however, its existence was inferred and

(29) Audier, H. E.; Berthomieu, D.; Morton, T. H. *J. Org. Chem.* **1995**, *60*, 7198–7208.

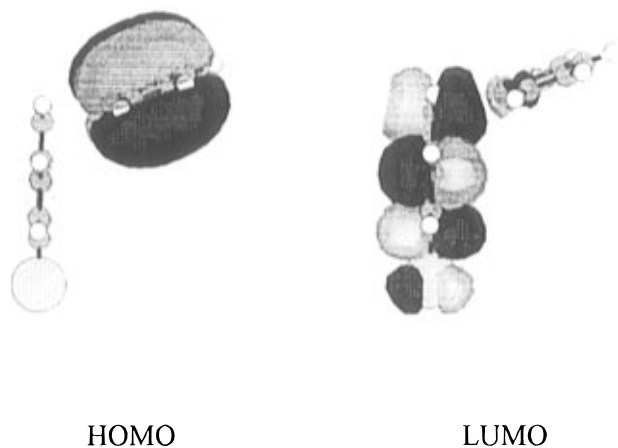
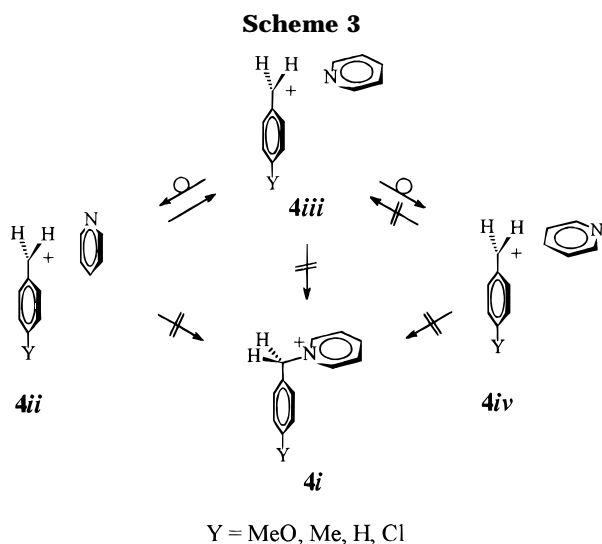


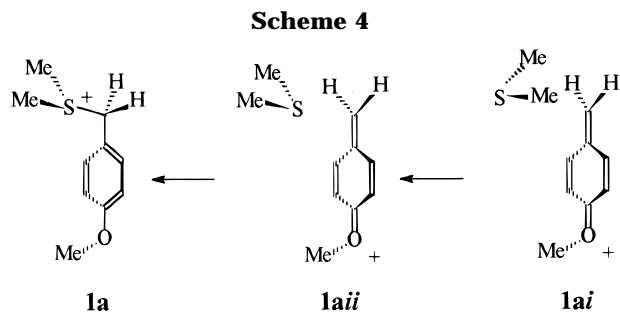
Figure 5. HOMO and LUMO for **2d** displayed in the ChemPlus option of Hyperchem for the AM1-minimized structure. The LUMO of the carbenium ion has the same structure as the INC.



ascribed to an entropic rather than an enthalpic bottleneck. As noted above, our semiempirical results are consistent with the existence of structures for both bottlenecks on the potential energy surface.

The molecular orbital picture for these species is consistent with an INC as well. In the four stable structures for **4a–d**, the HOMO is localized on the pyridine, while the LUMO is localized on the carbenium ion (Figure 5 for the **4d** INC). The LUMO in the INC has the same shape found in the respective carbenium ions, although there is slight delocalization into the pyridine, which is consistent with polarization of the neutral by the carbenium ion.

Arguing by analogy can be dangerous, *but* in this instance there are very clear correspondences between the experimental and computational results for the gas-phase dissociation of the 2'-substituted β -nicotinamide arabinosides and **2–5a–d** that appear to react through an INC.² First, the relative rates for both series follow LFERs. Second, both show excellent correlations between the experimental rate constants and the computed values for the various relevant computed ΔH^\ddagger and ΔH_R values (not shown). Third, INCs are stable upon minimization. Fourth, both the arabinosides and the benzylpyridiniums have the HOMO localized on the pyridine moiety; in the arabinosides, the LUMO is localized on the oxocarbenium ion moiety and partially on the pyri-



dine, but in the benzyls it is localized almost entirely on the carbenium ion. Thus, with the exception of the inability of the benzyl INCs to undergo proton transfer, the rate-energy correlations and molecular orbital pictures are virtually identical in the two systems. While this strong correspondence does not constitute proof that both systems react by the same mechanism, it strengthens the arguments in favor of the INC mechanism for the benzylpyridiniums.

As noted above, there is not sufficient experimental evidence available to speculate about the mechanism of dissociation for the dimethylsulfonium substrates. The Hammett plot is linear (Figure 1), which suggests that the mechanism is the same across the series, but this would fit any of the schemes considered above for the pyridiniums. The value of ρ^+ , -0.6 , is 2-fold greater than the value of ρ^+ for the pyridiniums (-0.24 to -0.35), suggesting that there is much more "carbenium ion character" in the activated complex for the sulfoniums (later transition state in Hammond terms). Semiempirical results provide some insight, however. The energy profiles for **1a–e** calculated in PM3 or AM1 (not shown) do not have distinct transition states, and there are no stable structures corresponding to INCs on the potential energy surface. In fact, removing the constraint on structures with benzyl-SMe₂⁺ bond lengths as great as 5 Å and minimizing leads to spontaneous collapse to the starting structure. This result is not surprising given the softness of both the carbenium ion and SMe₂. If the SMe₂ is rotated 180° about its center of mass to give a structure (**1ai**) in which the Me's shield the S and the structure is minimized in AM1, unlike the equivalent benzylpyridine structure shown above it collapsed directly back to the starting structure through the "locked rotor" structure **1aii** (Scheme 4). Thus, for the sulfoniums, stable structures corresponding to neither entropic nor enthalpic bottlenecks are identified computationally. In this context, the lack of break in the Hammett plot, the higher value of ρ^+ , and the semiempirical results are consistent with but do not prove the existence of a direct dissociation mechanism (k_d in eq 1).

Dissociation in Water. Unlike the corresponding plot for the gas-phase results, the Hammett plot (vs σ^+) for the hydrolysis in pure water (no added salt) of a series of 3- and 4-substituted benzyl dimethylsulfonium substrates^{5,30} shown in Figure 6 has the break between **1a** and **2a** typically found for the solvolysis and substitution reactions of neutral benzyl substrates.³¹ It was reported recently^{5,8} that this break is the result of a change in

(30) Friedberger, M. P.; Thornton, E. R. *J. Am. Chem. Soc.* **1976**, *98*, 2861–2865.

(31) See, for example: Fujio, M.; Goto, M.; Susuki, T.; Akasaka, I.; Mishima, M.; Tsuno, Y. *Bull. Chem. Soc. Jpn.* **1990**, *63*, 1146–1153. Reference 48 has an extensive review of studies on the substitution reactions of benzyl derivatives.

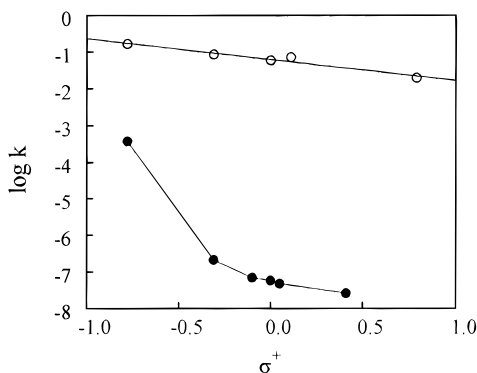


Figure 6. Plots of the gas-phase relative rates ($k = R^+/[R^+ + M^+]$, ○) for **1a–e** and the hydrolysis rate constants k_{obsd} at 70 °C for **1–c** and the (3-methylbenzyl)- and (3-bromobenzyl)-dimethylsulfonium compounds from ref 30 (●) vs σ^+ . For the gas-phase data, $\rho^+ = -0.57$ ($r = 0.9999$ with the point for Cl excluded). For the hydrolysis data, $\rho^+ = -7.7$ for the regression line between **1a** and **1b** and $\rho^+ = -0.82$ ($r = 0.993$) for the compounds with $\sigma^+ > -0.06$.

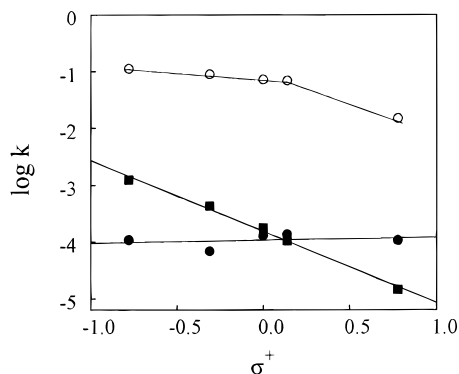


Figure 7. Plots of the gas-phase relative rates ($k = R^+/[R^+ + M^+]$, ○) for **2a–e** and the hydrolysis rate constants k_{obsd} at 70 °C for **2a–e** (■) and **3a–e** (●) vs σ^+ . For the gas-phase data for **2a–d**, $\rho^+ = -0.24$ ($r = 0.998$), which is one-half the value for **1a–e** (Figure 6). For the hydrolysis data, $\rho^+ = -1.25$ ($r = 0.997$) for **2a–e** and 0 for **3a–e**.

mechanism from S_N1 for the 4-MeO compound (a “ k_C ” process) to S_N2 (a “ k_S ” process) for compounds with 4-substituents with $\sigma^+ > -0.31$. Unlike the corresponding plot for the gas-phase results, the Hammett plot based on estimated rate constants for **2a–e** is linear with a slope ($\rho^+ = 1.25$) and for **3a–e** the Hammett plot is linear and flat ($\rho^+ \sim 0$, Figure 7), consistent with a single k_S mechanism. (Reasons for the difference in slopes for the pyridiniums are discussed elsewhere⁶ in terms of Pross–Shiak theory.³²) The fact that both plots are linear shows that the structure of the activated complex changes constantly and smoothly as a function of substituent, unlike the recent results of Richard and Yeary³³ for the reaction of azide with benzyl bromides that is marked by curvature resulting from nonsynchronous resonance demand in the activated complex. (The fact that the Hammett plots for the second-order rate constants for the azide reactions of the benzyl dimethylsulfoniums is a smooth curve³⁴ (concave up) and that the plots for the azide reactions of **2–4a–e** change shape

from flat and linear to V-shaped suggests that the charge on the substrate and the nucleophile, and the HSAB rank of the nucleophile, has a significant influence on the structure of the activated complex.) Despite the borderline kinetic behavior, there was no evidence for an IDC in any system; in fact, rate and selectivity data for **1a** show unequivocally that an IDC is not involved.^{4,5,8} These pronounced differences between the solution and gas phases show that it is not always wise to assign a mechanism to one phase based on a mechanism in another.

Implications for the Solution Reactions of the Relative Stabilities of the Ribosyl Oxocarbenium and (4-Methoxybenzyl)carbenium Ions in the Gas Phase.

All evidence, including high values of the Taft ρ_T ,^{1,3} high, negative Brønsted β_{LG} values,³⁵ and positive ΔS^\ddagger values,³⁶ points to a well-behaved dissociative reaction for NAD^+ and 2'-substituted β -nicotinamide arabinosides and ribosides that may occur through an IDC in water^{3,37} and an INC in the gas-phase.² A large body of historical evidence^{38–40} is consistent with an A-1 mechanism for the specific acid-catalyzed hydrolysis of methyl and other alkyl glucosides⁴⁰ and acetals and ketals formed from “normal” aldehydes, ketones, and aliphatic alcohols.⁴¹ There is similar evidence that glycosylpyridiniums react through a dissociative mechanism.⁴² In a very recent study, Bennet and colleagues⁴³ showed that 2-deoxy- β -D-glucosylpyridiniums react with nucleophiles ($s \sim 0$) through a dissociative mechanism, with nucleophile trapping at the solvent-separated ion pair. These results require that ribosyl- and glucosyloxocarbenium ions are intermediates, either as solvent-equilibrated species or as elements of IDCs.

Despite this historical evidence, for some years Jencks argued that the glycosyloxocarbenium ion was too unstable to exist as an intermediate in either solvolysis⁴⁴ or acid-catalyzed hydrolysis^{45,46} of glucosyl substrates. The initial Young–Jencks⁴⁵ estimate of the lifetime of the glycosyl oxocarbenium ion, 10^{-15} s, has been revised downward over the years to 10^{-12} s.⁴⁶ On the basis of a study of the nucleophilic substitution reactions of α -D-glucopyranosyl fluoride, Banait and Jencks⁴⁷ concluded that the the glycosyloxocarbenium ion has a finite lifetime in solution but that it does not become solvent equilibrated and has no significant lifetime in contact with a strong nucleophile.

(34) While the reaction of **1e** with azide was studied only cursorily, the rate constants for reaction with 2 M NaN_3 are much lower than those for **1a**, which shows that the Hammett plot is not V-shaped as found for the benzylpyridiniums. Buckley, N. Unpublished results.

(35) Tarnus, C.; Schuber, F. *Bioorg. Chem.* **1987**, *15*, 31–42. Tarnus, C.; Müller, H. M.; Schuber, F. *Ibid.* **1988**, *16*, 38–51.

(36) Handlon, A. L. Ph.D. Dissertation, The University of California, San Francisco, 1991.

(37) Ta-Shma, R.; Oppenheimer, N. J. Unpublished results.

(38) Schaleger, L. L.; Long, F. A. *Adv. Phys. Org. Chem.* **1963**, *1*, 1–34.

(39) Bunnett, J. F. *J. Am. Chem. Soc.* **1961**, *83*, 4956–4968; 4968–4973; 4973–4978; 4978–4983.

(40) Capon, B. *Chem. Rev.* **1969**, *69*, 407–498.

(41) Cordes, E. H.; Bull, H. G. *Chem. Rev.* **1974**, *74*, 581–603.

(42) Hosie, L.; Marshall, P. J.; Sinnott, M. L. *J. Chem. Soc., Perkin Trans. 2*, **1984**, 1121–1131.

(43) Huang, X.; Surry, C.; Hiebert, T.; Bennet, A. J. *J. Am. Chem. Soc.* **1995**, *117*, 10614–10621.

(44) Sinnott, M. L.; Jencks, W. P. *J. Am. Chem. Soc.* **1980**, *102*, 2026–2032.

(45) Young, P. R.; Jencks, W. P. *J. Am. Chem. Soc.* **1977**, *99*, 8238–8248.

(46) Amyes, T. L.; Jencks, W. P. *J. Am. Chem. Soc.* **1989**, *111*, 7888–7900.

(47) Banait, N. S.; Jencks, W. P. *J. Am. Chem. Soc.* **1991**, *113*, 7951–7958.

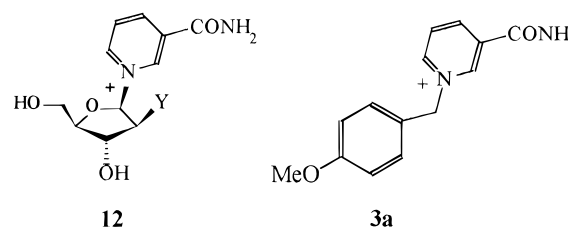
(32) Pross, A. *Adv. Phys. Org. Chem.* **1985**, *21*, 99–195.

(33) Richard, J. P.; Yeary, P. E. *A Simple Explanation for Curved Hammett Plots for Nucleophilic Substitution Reactions at Ring-Substituted Benzyl Derivatives*; presented at the 206th ACS National Meeting, Chicago, IL, 22–27 Aug, 1993.

1–3a all have the same potential intermediate, the (4-methoxybenzyl)carbenium ion that is known to be a solvent-equilibrated intermediate in highly aqueous solvent systems.^{5,8,48} These substrates, however, exhibit the full range of possible mechanisms for the reaction with azide in water under identical conditions: **1a**, mixed S_N1/S_N2 with comparable rates for both pathways;^{5,8} **2a**, direct displacement by both azide and water,⁶ with the rate for the water reaction much slower than the azide reaction ($k_{\text{rel}} = 4 \times 10^3$); **3a**, direct displacement by both azide and water that occur at comparable rates—typical borderline kinetic behavior. Despite the fact that the pK_a's of the LGs for **1a** and **2a** differ by 7–8 units, the second-order rate constants for the azide reaction at 80 °C under identical conditions differ only by a factor of 2.5. ΔH^\ddagger is 4.6 kcal/mol lower for **2a** than for **1a**, but ΔS^\ddagger is 15 gibbs/mol more positive for **1a**, the result of different solvation of the LGs in the activated complex.⁵ This large difference in ΔS^\ddagger is apparently the source of the inability of **2a** to undergo an S_N1 reaction.⁶ There was no evidence for ion pairs under conditions of constant ionic strength in any system. Thus, by merely changing the LG in substrates with the same putative stable, potentially solvent-equilibrated carbenium ion,^{5,8,48} both relative rates and mechanism change. In the benzyl series at least, solvation is much more important than the stability of the putative intermediate. While it is of course true, as Jencks has contended for many years,⁴⁹ that a substrate that cannot generate a stable intermediate is “forced” to undergo a concerted displacement reaction, the mere presence of a potentially stable intermediate in a substrate does not guarantee that a stepwise mechanism will be followed in a solvolysis or nucleophilic substitution reaction.⁵⁰

The ground states and activated complexes for the benzyl and arabinosyl and ribosyl substrates will be solvated to much different extents, which makes a direct comparison of results among the series risky at best. Nonetheless, certain patterns are apparent. Despite the unfavorable entropy of solvation of the LG, the β -nicotinamide ribosides and arabinosides appear to undergo fully dissociative reactions,^{1,3,35–37,51} which suggests in turn that in this instance the stability of the oxocarbenium ion is sufficient to overcome the negative driving force of solvation entropy. Handlon found that addition of exogenous nicotinamide did not affect the rate of hydrolysis of several of the substrates.³⁶ The lack of a common LG effect rules out a solvent-equilibrated oxocarbenium ion as an intermediate, but is consistent with a solvent-separated IDC, which in turn is consistent with structures seen by Schröder *et al.*,⁵¹ in a computational study of the hydrolysis of β -nicotinamide riboside, and with selectivity and rate patterns seen by Ta-Shma and Oppenheimer³⁷ in a study of the solvolysis and azide substitution reactions of NAD⁺ in methanol–water mixtures. In Bennet's recent study⁴³ of glucosyl pyridinium hydrolysis and nucleophilic substitution reactions, a

Chart 2



solvent-separated IDC was shown to be the intermediate from which product formed.

Thus, the combination of solvent and LG effects makes comparison of solution data as a measure of the relative stabilities of carbenium ions extremely difficult. The relative *intrinsic* gas-phase stabilities of the ribosyl oxocarbenium ion and the (4-methoxybenzyl)carbenium ion derived from arabinosyl compounds and **3a** can be compared directly from our data (Chart 2). For instance, $R^+/[R^+ + M^+]$ for 2-deoxyribose- β -nicotinamide (**12**), which forms the most stable carbenium ion in Handlon's series,^{2,3} is 0.24, while that for **3a** is 0.10. The AM1-calculated ΔH^\ddagger for the carbon–nicotinamide cleavage² is 20.1 kcal/mol for **12** and 30.1 kcal/mol for **3a**. The corresponding values for the 2'-F-arabinoside, which forms the least-stable oxocarbenium ion in the arabinosyl series, are 0.11 and 26.0 kcal/mol, respectively. The same trend is found in ΔH_R^\ddagger ; for **3a** the value is 34.6 kcal/mol, while the values for 2'-H-, 2'-NH₂-, 2'-OH-, 2'-NAc-, and 2'-F-arabinosyl β -nicotinamide compounds, listed in the order of decreasing stability of the oxocarbenium ions, are 27.5, 29.8, 32.7, 33.3, and 37.9 kcal/mol, respectively. Thus, with nicotinamide as the LG, in the gas phase the ribosyl INCs and oxocarbenium ions form at faster rates than the quite stable 4-MeO-benzyl INCs and carbenium ions. By this measure, the intrinsic stabilities of the ribosyl oxocarbenium ions within the INC, and the bare species that remain after diffusion away of the LG, are greater than the (4-methoxybenzyl)carbenium ion. Even by the Young–Jencks rate comparison criterion,⁴⁵ the same trend is found in solution: the k_{rel} for hydrolysis of **12** and **3a** is 6.4×10^4 at 96 °C in favor of **12**. This comparison of solution rate constants is invalid, however, because **12** appears to solvolyze through an IDC,^{36,37} while **3a** solvolyzes by direct solvent displacement.⁶

One consequence of this stability and the effect of solvent can be seen readily in the reactions of substrates in enzyme active sites. Shuber and his colleagues³⁵ suggested that the difference between the selectivity $k_{\text{MeOH}}/k_{\text{HOH}}$ for the solvolysis ($k_{\text{MeOH}}/k_{\text{HOH}} = 2$) and enzyme-catalyzed reactions ($k_{\text{MeOH}}/k_{\text{HOH}} = 100$) of NAD⁺ analogs was the result of the much greater selectivity of a fully formed, stable ribosyl oxocarbenium ion in the active site of the enzyme. This contention was recently confirmed by a structure–activity study in the same enzyme.^{1b} Richard and his colleagues⁵² have recently reached a similar conclusion for β -galactosidase, an enzyme that yields a galactosyl oxocarbenium ion in the active site that gives $k_{\text{MeOH}}/k_{\text{HOH}} = 130$. Consistent with the gas-phase stabilities, these results show that both ribosyl- and pyranosyloxocarbenium ions appear to be stable intermediates in enzyme active sites.

Thus, rate and structure–activity data are mediated by a complex interaction of solvent (ΔH^\ddagger and ΔS^\ddagger), leaving

(48) Amyes, T. L.; Richard, J. P. *J. Am. Chem. Soc.* **1990**, *112*, 9507–9512.

(49) Jencks, W. P. *Acc. Chem. Res.* **1980**, *13*, 161–169. Jencks, W. P. *Chem. Soc. Rev.* **1981**, *10*, 345–375.

(50) The last sentence of Knier, B. L.; Jencks, W. P. *J. Am. Chem. Soc.* **1980**, *102*, 6789–6798, states that “[A]ll solvolysis and substitution reactions at saturated carbon that proceed through S_N2 displacement mechanisms do so simply because the intermediate in the alternative S_N1 mechanism is too unstable to exist [italics added].”

(51) Schröder, S.; Buckley, N.; Oppenheimer, N. J.; Kollman, P. A. *J. Am. Chem. Soc.* **1992**, *114*, 8231–8238.

(52) Richard, J. P.; Westerfeld, J. G.; Lin, S.; Beard, J. *Biochemistry* **1995**, *34*, 11713–11724.

group (primarily ΔS^\ddagger), and substrate charge (differences in solvation of ground state and activated complex depending on charge) effects that are often difficult to sort out. In the absence of gas-phase results, attempts to assess these data in terms of the stability of the intermediate may lead to entirely reasonable interpretations; if the intrinsic stabilities are known from gas-phase studies, however, solution data may be interpreted considering the range of possible interactions and effects.

Acknowledgment. Supported in part by NIH Grant GM-22982 (N.J.O.), a Biotechnology Grant from the

State of California (N.J.O., N.B.), and a Research Award from the UCSF Graduate Division (N.B.). Funds for the purchase and support of the tandem spectrometer in the UCSF Mass Spectrometry Facility (A. L. Burlingame, Director) were provided by a grant from the Division of Research Resources of the NIH (RR 01614) and a grant from the NSF (DIR 8700766). We thank Randy Radmer, Jim Caldwell, and Peter Kollman (UCSF) for helpful discussions concerning semiempirical calculations and the two reviewers for their insightful comments on the manuscript.

JO951257W